Boron Abundances in Diffuse Interstellar Clouds

Adam M. Ritchey
Department of Physics & Astronomy
The University of Toledo

IAU Symposium 268

Outline of Talk

Introduction to Interstellar Boron

- Motivation/Previous Work

STIS Observations/Data Reduction

- Archival Survey
- Extraction Issues
- The Boron Sample

Column Density Analysis

- Profile Synthesis

Results on Interstellar Abundances

- Depletion onto Dust Grains
- Galactic Evolution of Boron
- Enhanced Boron Abundances

Conclusions/Future Work

Previous Detections of Interstellar Boron

Meneguzzi & York (1980): first detection of interstellar boron (via the B II resonance line at 1362.46 Å in *Copernicus* observations of κ Ori).

→ interstellar abundance, log ε(B) = 2.2 ± 0.3, consistent with the stellar value, 2.3 ± 0.3 (Boesgaard & Heacox 1978), assumed to be the galactic value.

> Further observations of the B II λ1362.46 resonance line are required along different lines of sight to establish the B/H interstellar value and to test the hypothesis of the production of B and Be by cosmic rays in the interstellar medium. A general study seems beyond the reach of the present UV instruments, but could be done with the Space Telescope.

Meneguzzi & York 1980

Jura et al. (1996): found that boron abundances toward Orion (from GHRS spectra) were consistent with an earlier measurement toward ζ Oph (Federman et al. 1993). Since all were a factor of 4 less than the solar value, a scenario either involving metal-poor infall or depletion onto grains was proposed.

Previous Detections of Interstellar Boron

Federman et al. (1996), Lambert et al. (1998): first measurements of $^{11}B/^{10}B$ outside the solar system (again using GHRS).

→ mean value (3.4 ± 0.7) showed that the solar system ratio (4.0) was not anomalous but probably representative of the local Galactic neighborhood.

→ also, found a lower abundance toward ζ Oph, suggesting boron abundance correlates with $f(H_2)$ and $E(B-V)$.

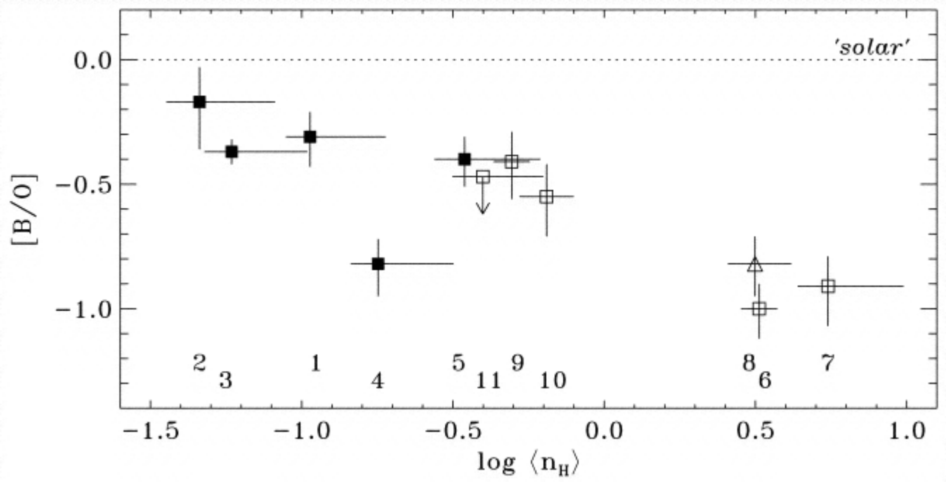

Howk et al. 2000

Howk, Sembach, & Savage (2000): expanded the sample of interstellar boron abundances (with STIS). Their sample strongly indicates that boron is depleted onto dust grains, which complicates the determination of the present-day total boron abundance in the ISM.

STIS Program to Measure $^{11}B/^{10}B$ near IC 348

Observed 4 stars in Per OB2 near the B II line: 40 Per, o Per, ζ Per, and X Per (GO 8622, PI: D. Lambert)

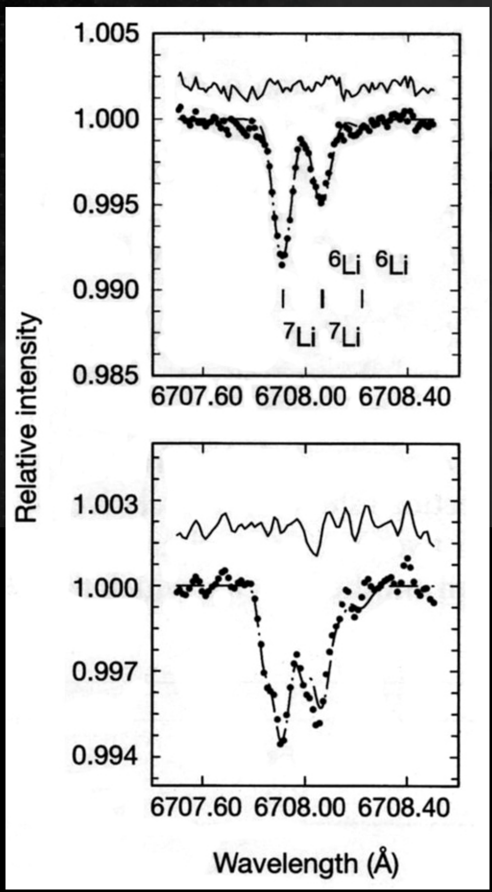

ζ Per:

$^7Li/^6Li$ = 10.6 ± 2.9

o Per:

$^7Li/^6Li$ = 1.7 ± 0.3
3.6 ± 0.6

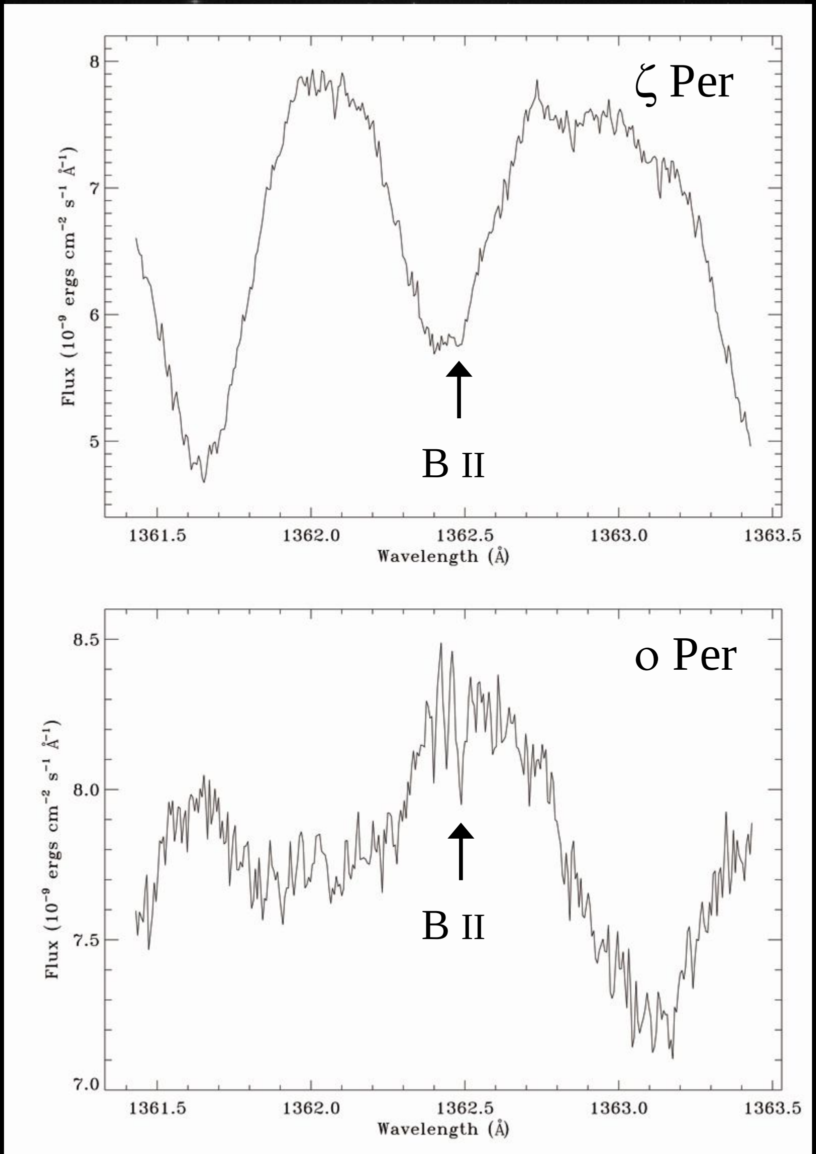

Knauth et al. 2000 (Nature; see also IAU Symp. 198)

STIS Archival Search

Examined all archival *HST*/STIS datasets employing the FUV MAMA detector and either the high-resolution (E140H) or medium-resolution (E140M) grating.

Searched for unambiguous absorption from the dominant ion species: O I λ1355, Cu II λ1358, and Ga II λ1414. O^0, Cu^+, and Ga^+ should coexist with B^+ in diffuse clouds.

→ subsequent searches for absorption from B II λ1362 resulted in detections along 56 Galactic sight lines (37 with E140H, 19 with E140M).

Image Credit: NASA

All STIS datasets for the final sample were retrieved from MAST after final close-out recalibration of STIS archival data, completed in 2007.

Extraction of FUV MAMA Edge Orders

STIS echelle spectrum of HD 43818:

FUV MAMA detector
E140H grating
central wavelength: 1271 Å

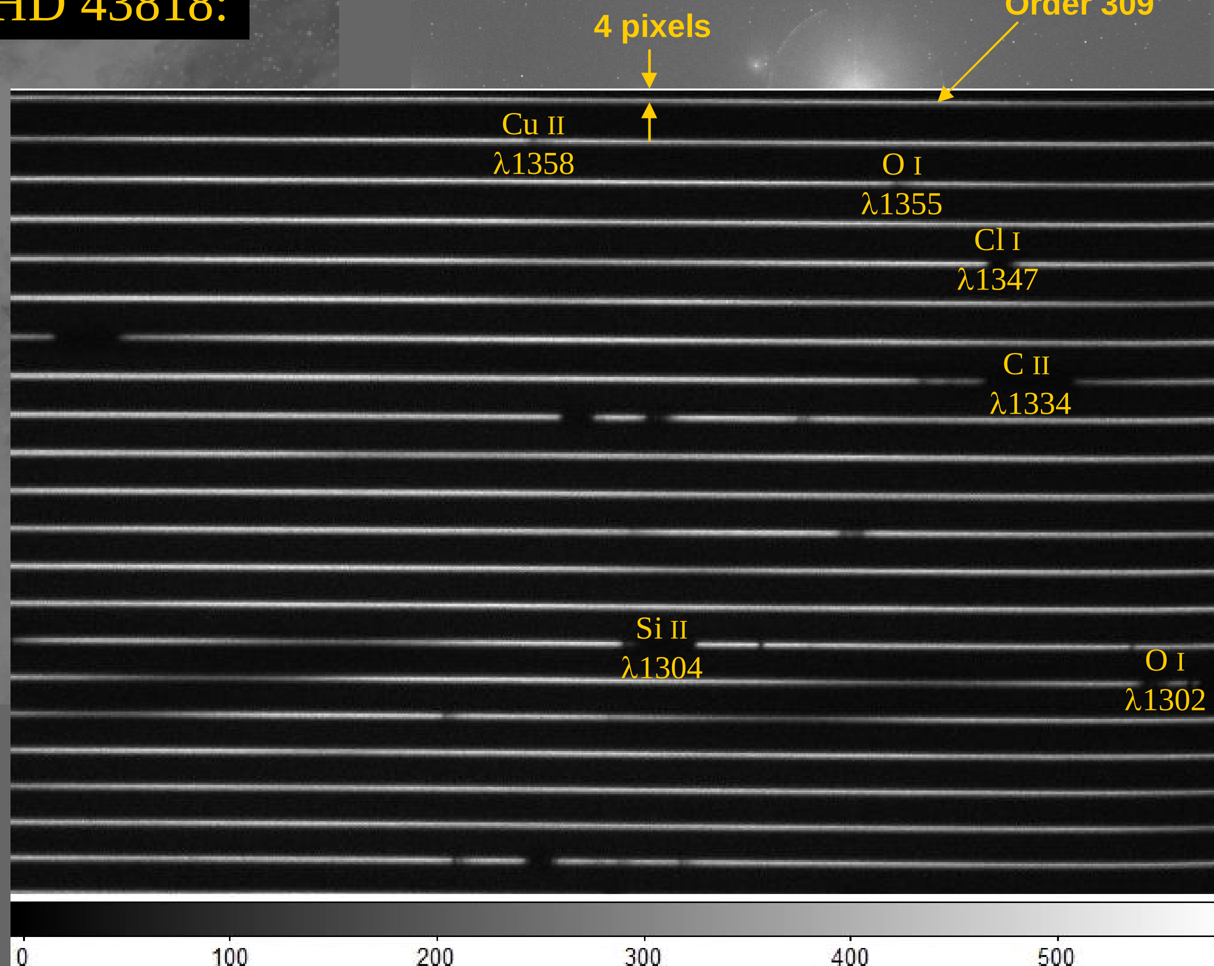

14 detections would not have been possible with standard CALSTIS pipeline reduction

Extraction of FUV MAMA Edge Orders

STIS echelle spectrum of HD 43818:

FUV MAMA detector
E140H grating
central wavelength: 1271 Å

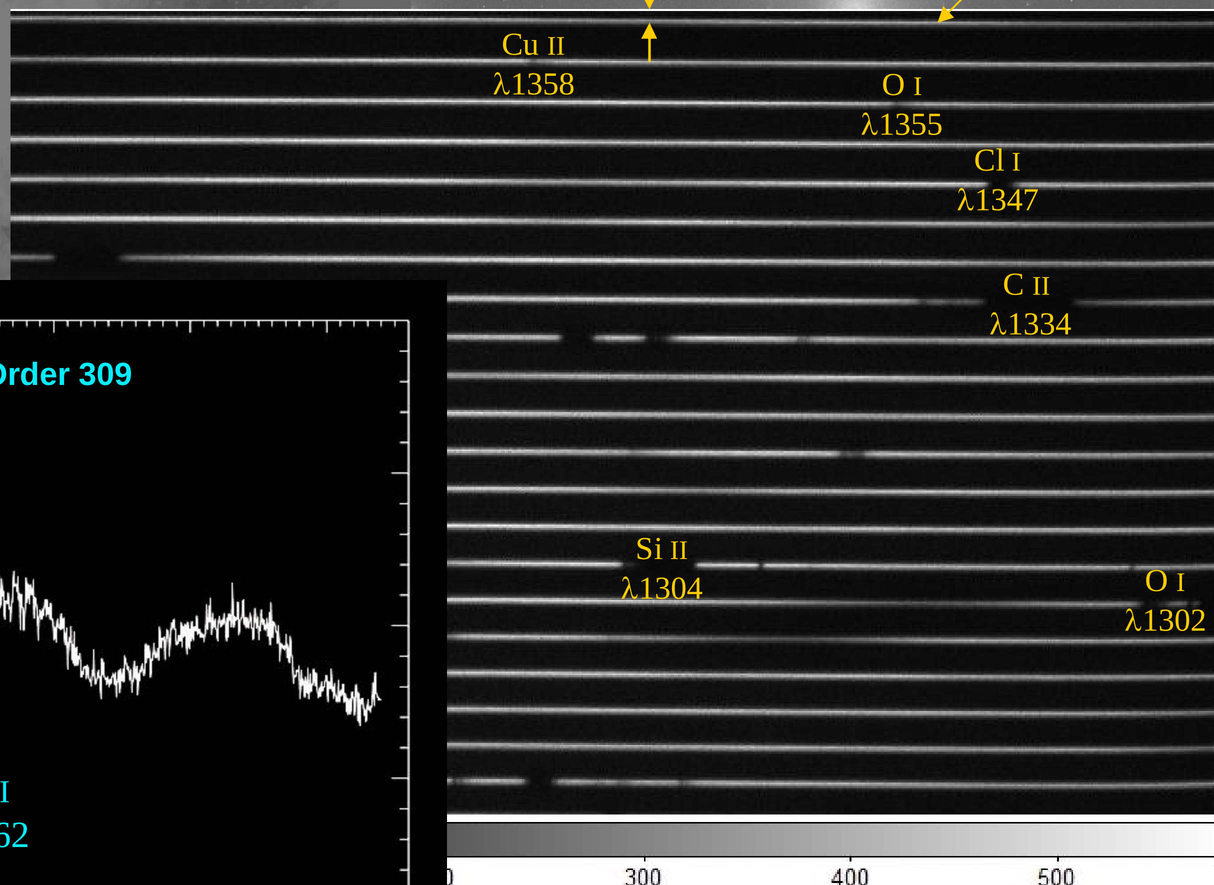

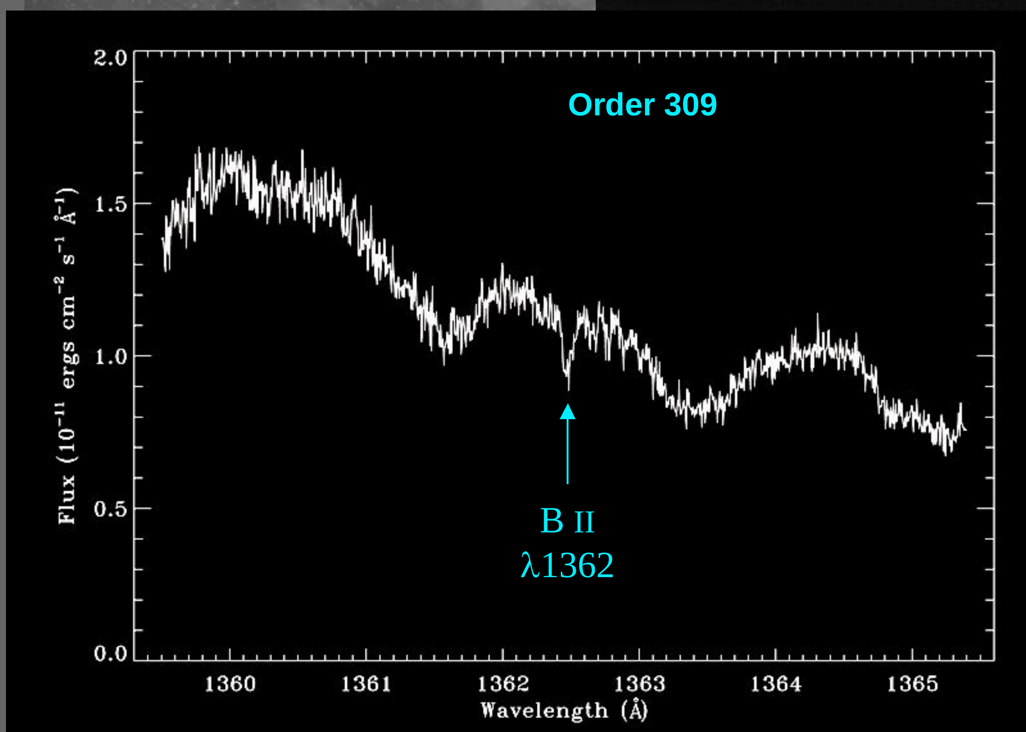

Distribution of Stars in the Boron Sample

Solar Neighborhood:

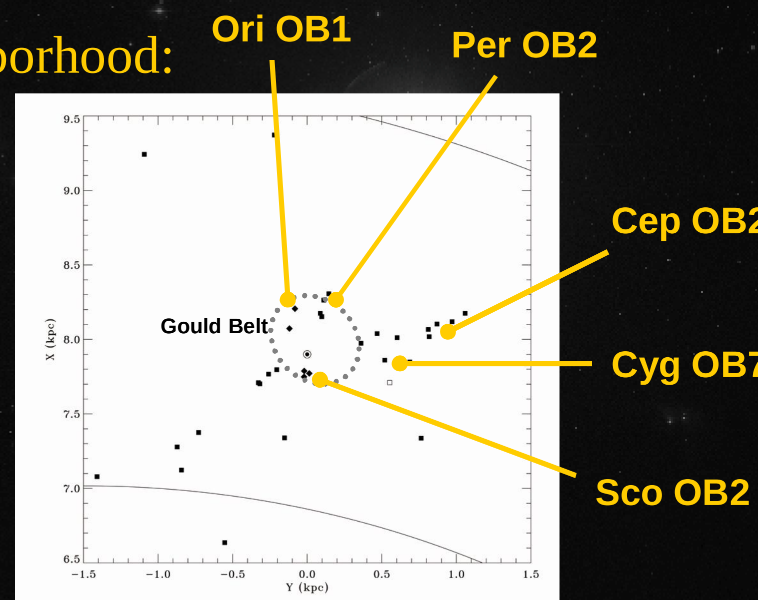

Galactic Distribution:

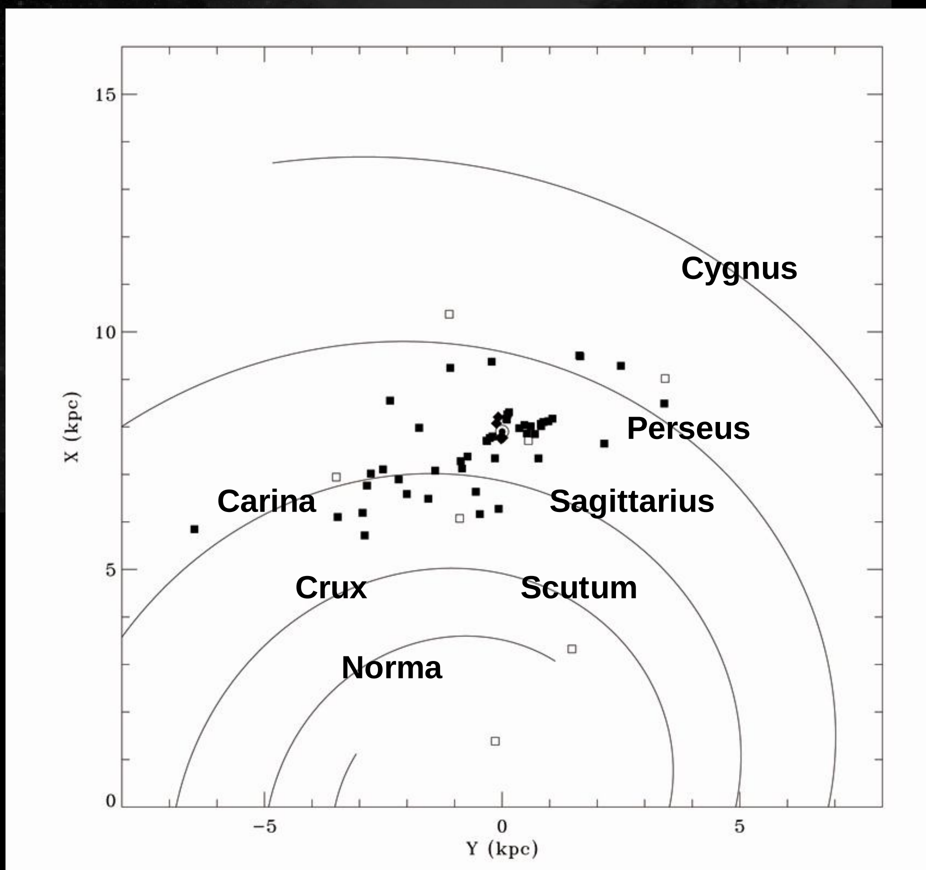

Halo Stars:

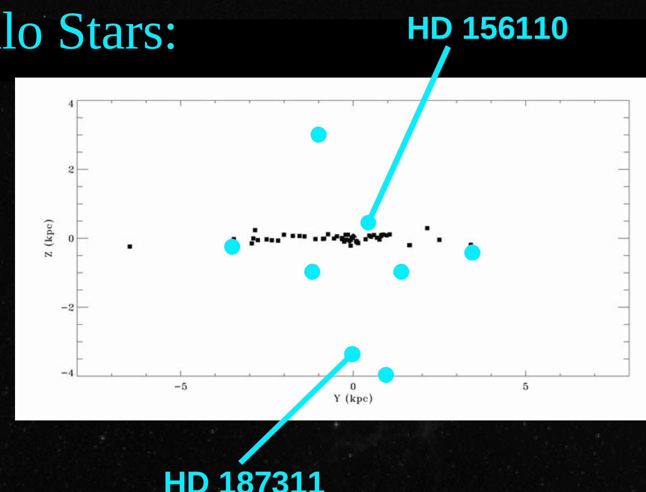

STIS Spectra

Examples of UV profiles (E140H):

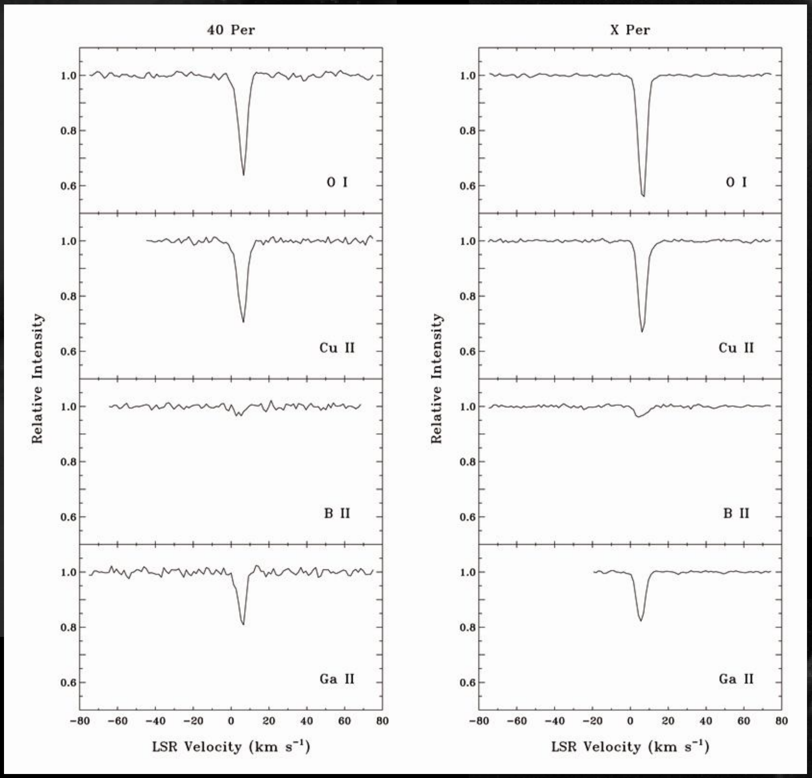

R = 82,000–143,000

Δv = 2.1–3.6 km s^{-1}

STIS Spectra

Examples of UV profiles (E140H):

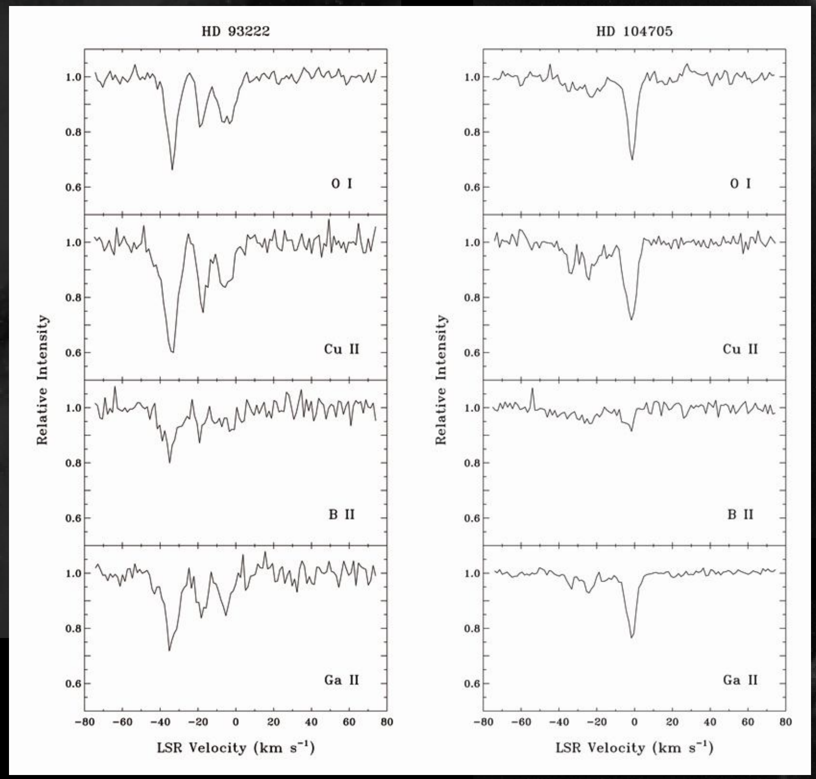

R = 82,000−143,000

Δv = 2.1−3.6 km s^{-1}

STIS Spectra

Comparison between high (E140H) and medium (E140M) resolution:

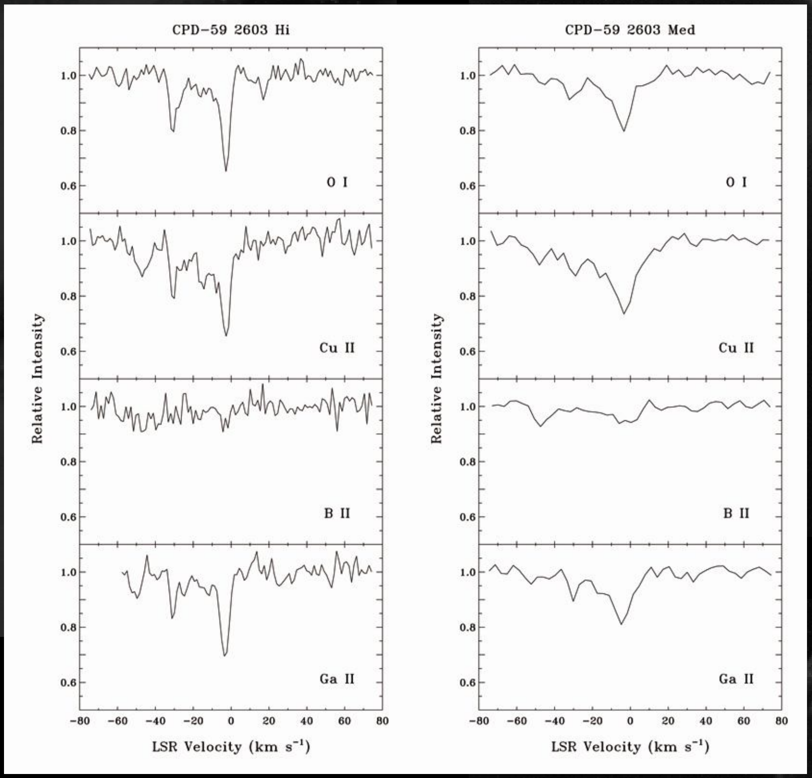

R = 108,000 Δv = 3.8 km s^{-1}

R = 38,000 Δv = 7.9 km s^{-1}

Ground-based McDonald Data

Ca II λ3933 and K I λ7698 profiles from McDonald Observatory 2.7 m:

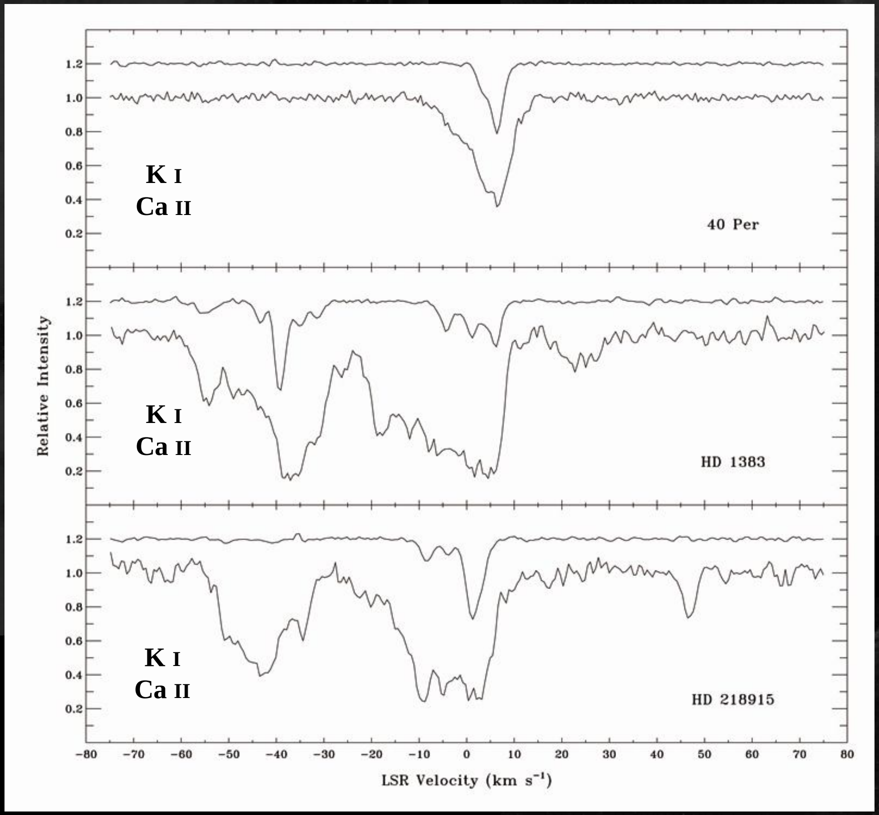

R = 165,000–185,000

Δv = 1.6–1.8 km s^{-1}

Profile Synthesis

UV Templates:

Absorption profiles of O I λ1355, Cu II λ1358, and Ga II λ1414 were synthesized with the rms-minimizing code ISMOD (Y. Sheffer, unpublished).

→ yielded column density, *b*-value, and velocity of each absorption component along the line of sight.

→ results from these species served as fixed templates of component structure for fitting the B II line.

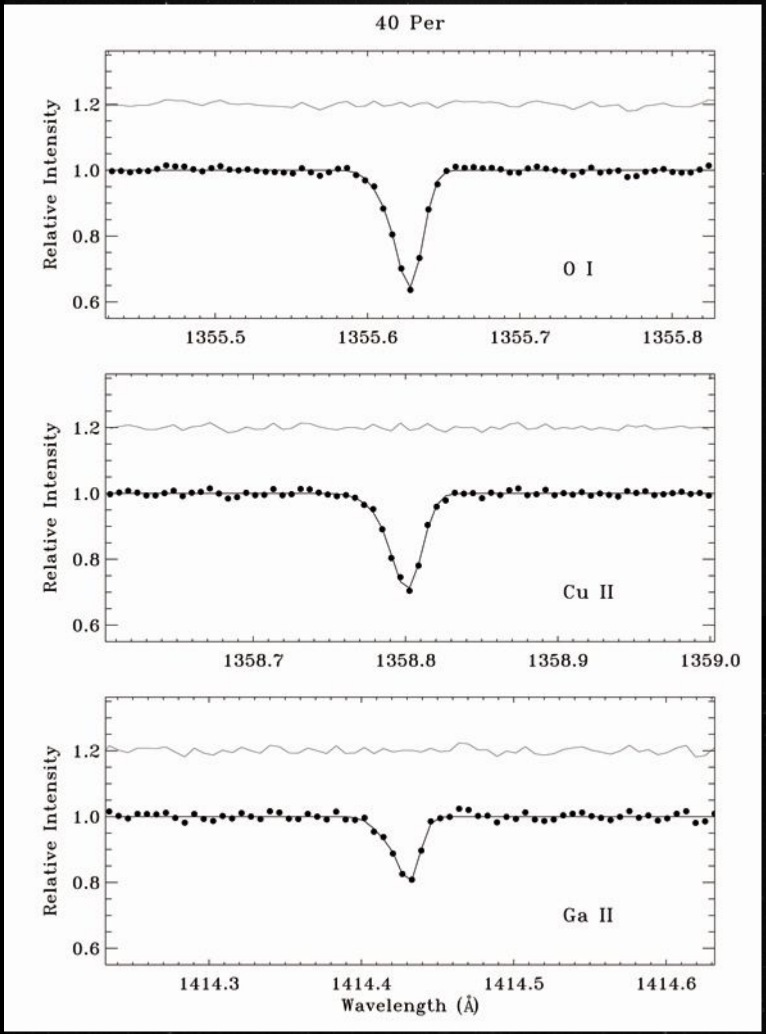

Profile Synthesis

Template from Visible Data:

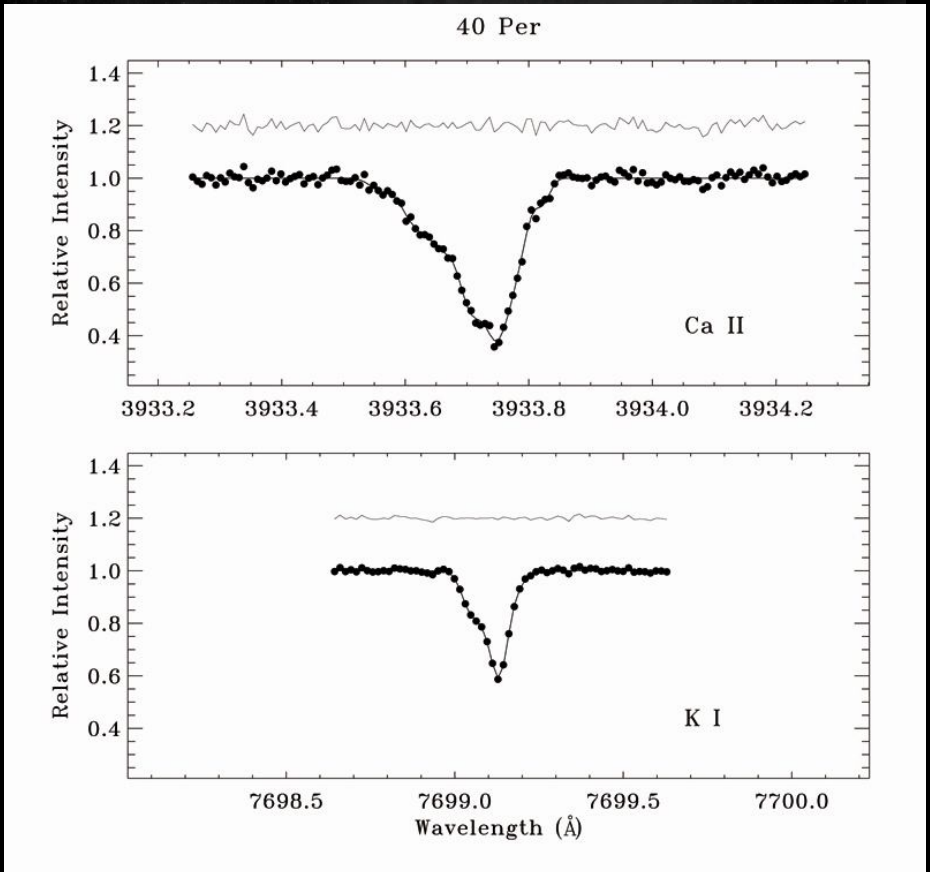

Ca II λ3933 and K I λ7698 profiles acquired at McDonald Observatory or obtained from the literature (in studies of comparable resolution) were also synthesized.

→ velocities from K I, *b*-values and component fractions from Ca II K (for components seen in K I)

Profile Synthesis

Profile template fits to B II λ1362:

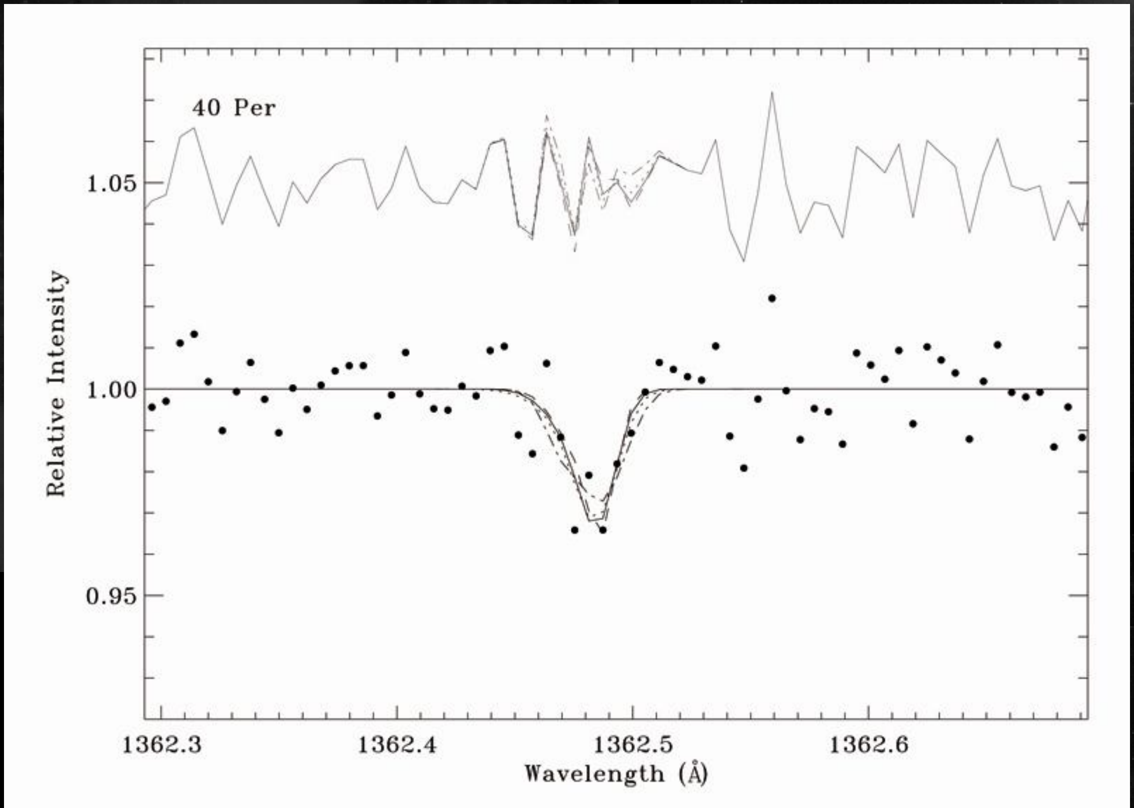

log N(B II) =

O I template:
10.69 ± 0.12

Cu II template:
10.72 ± 0.14

Ga II template:
10.66 ± 0.11

Ca II/K I template:
10.73 ± 0.13

Mean result:
10.70 ± 0.13

Profile Synthesis

Another example: Multiple complexes

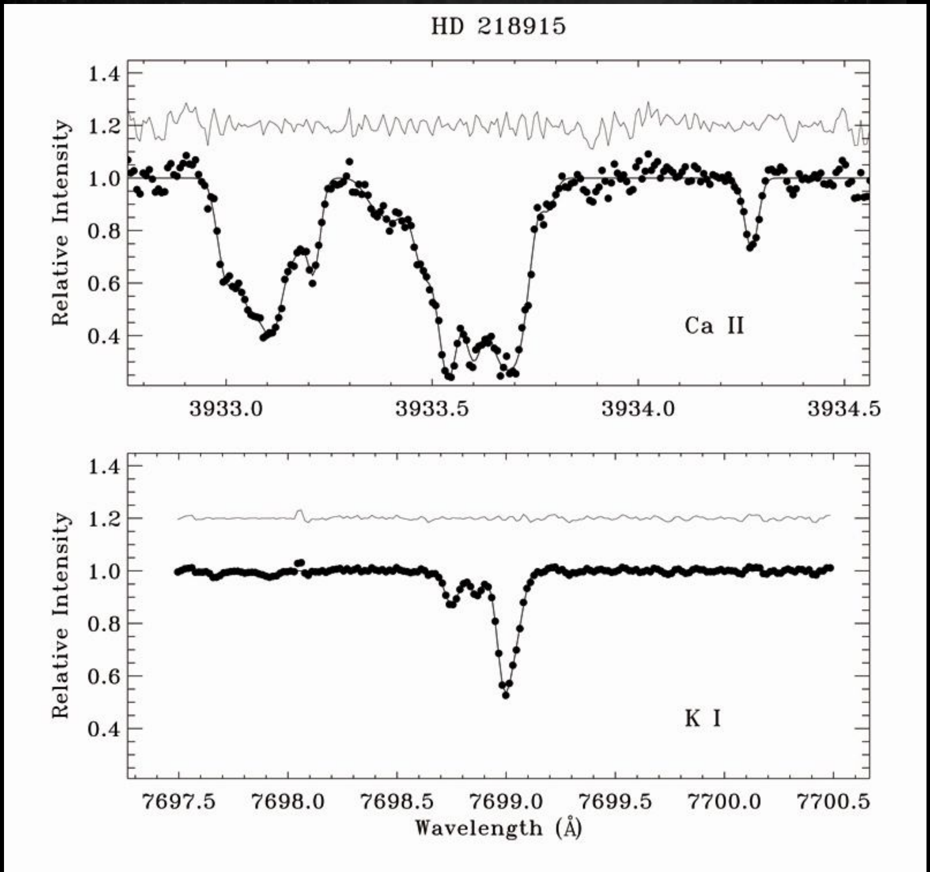

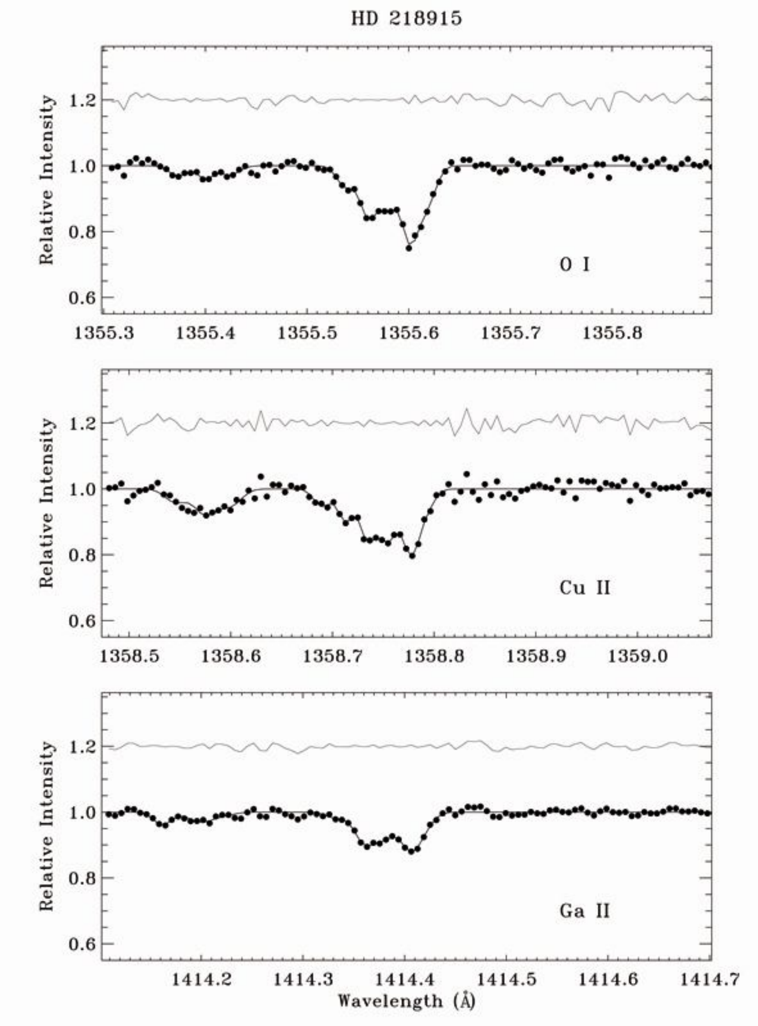

Profile Synthesis

Profile template fits to B II λ1362:

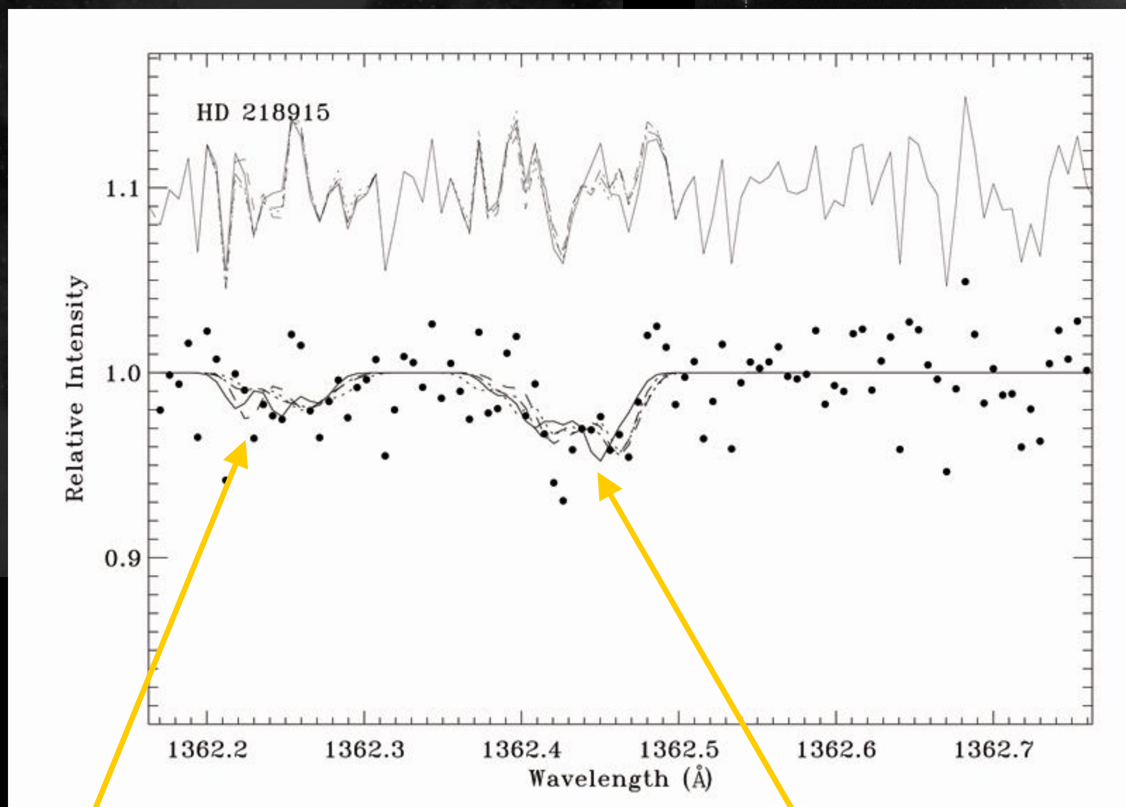

log N(B II) =

O I template:
11.38 ± 0.14

Cu II template:
11.39 ± 0.16

Ga II template:
11.39 ± 0.16

Ca II/K I template :
11.38 ± 0.18

Mean result:
11.38 ± 0.16

log (B/O) = −6.22

log (B/O) = −6.67

Profile Synthesis

Profile template fits to B II λ1362:

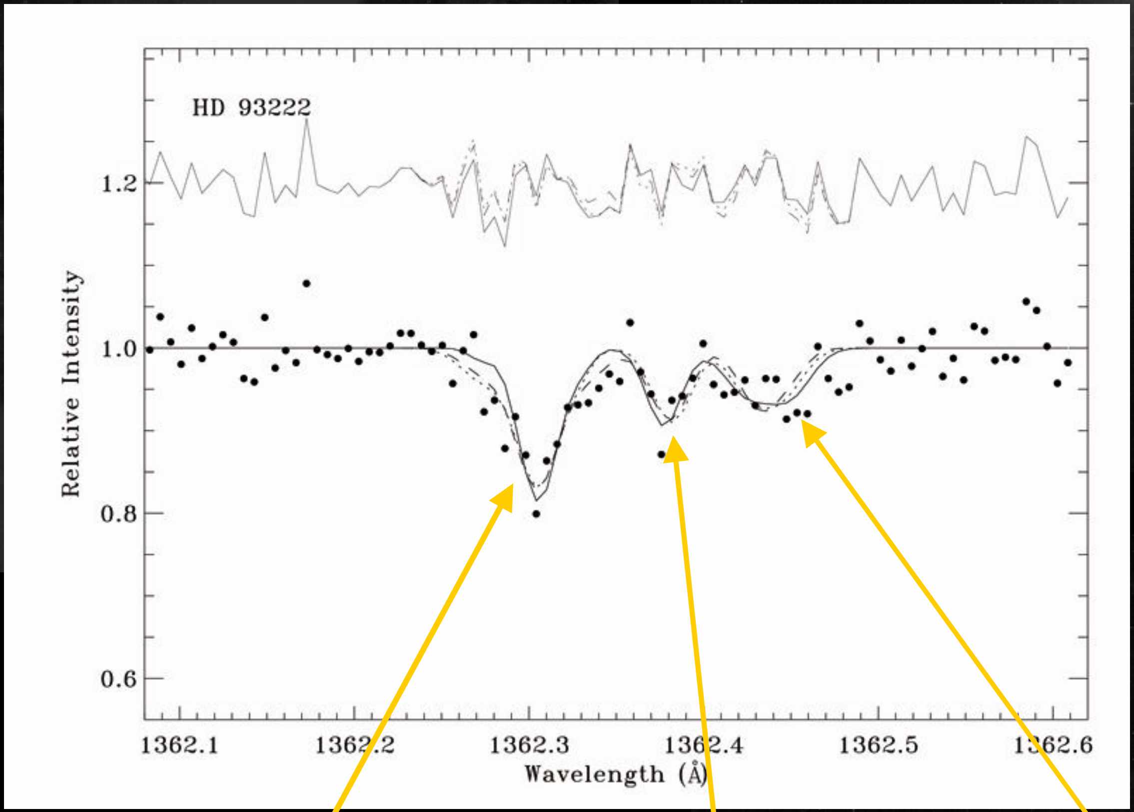

log (B/O) = −6.14

log (B/O) = −6.22

log (B/O) = −6.39

log N(B II) =

O I template:
11.88 ± 0.06

Cu II template:
11.90 ± 0.06

Ga II template:
11.90 ± 0.07

Mean result:
11.89 ± 0.06

Elevated B/O Ratios in Sagittarius-Carina?

Mean value of B/O for components at more negative velocities is 0.3 dex higher than for components near 0 km s^{-1}:

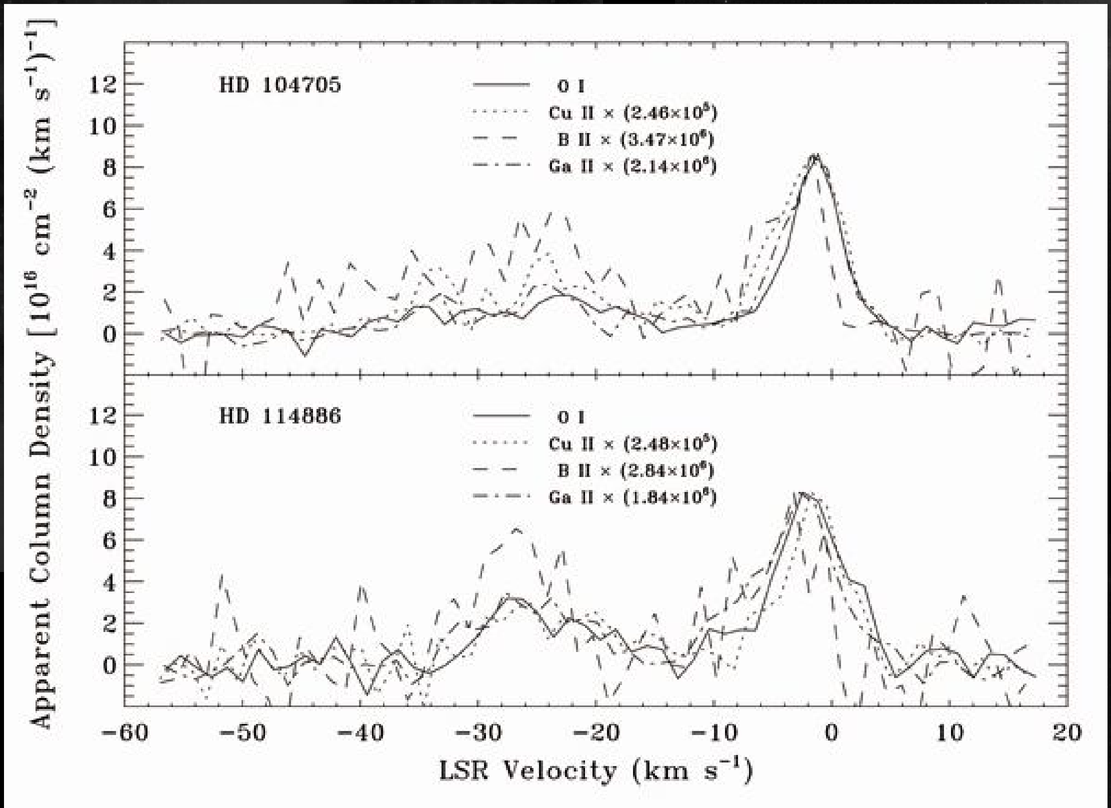

→ suggests boron behaves like other secondary elements, increasing in abundance relative to primary elements toward the Galactic center.

Signatures of Depletion

Increased depletion with increased average line-of-sight density and condensation temperature:

T_C = 180 K

T_C = 908 K

T_C = 968 K

T_C = 1037 K

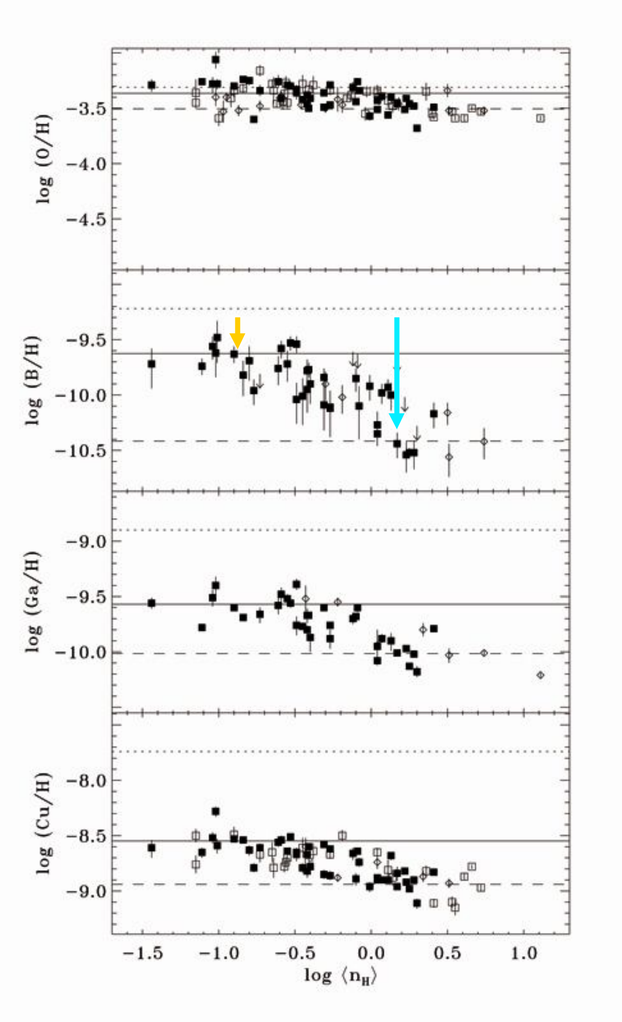

−0.05
−0.19

−0.40
−1.20

−0.67
−1.12

−0.81
−1.20

Signatures of Depletion

Increased depletion with increased average line-of-sight density
and condensation temperature:

T_C = 180 K

T_C = 908 K

T_C = 968 K

T_C = 1037 K

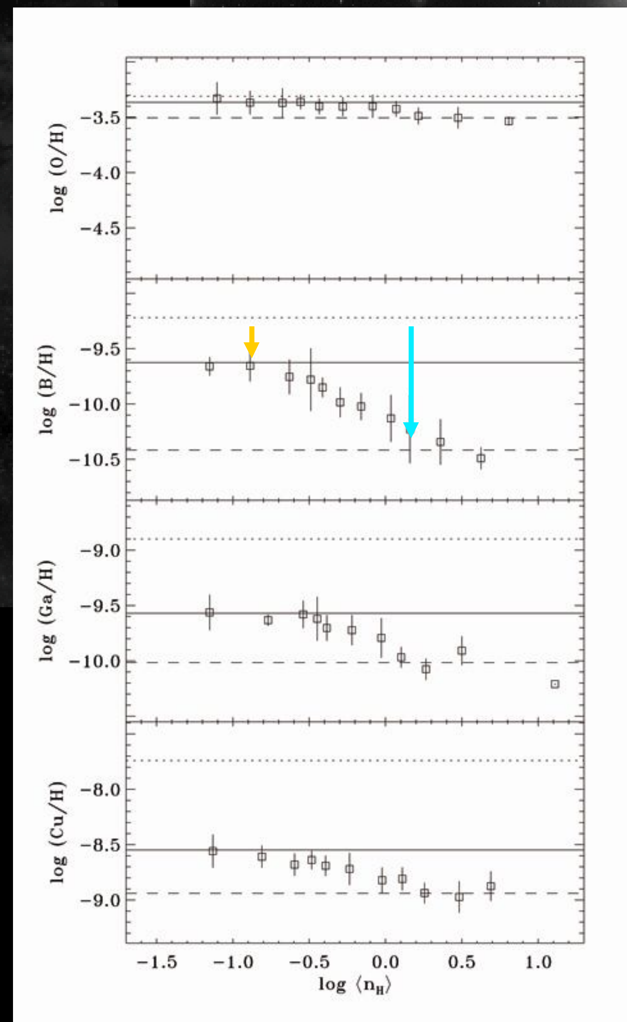

−0.05
−0.19

−0.40
−1.20

−0.67
−1.12

−0.81
−1.20

Signatures of Depletion

Constant abundance over 3 orders of magnitude in molecular fraction followed by precipitous drop at $f(H_2) = 0.1$:

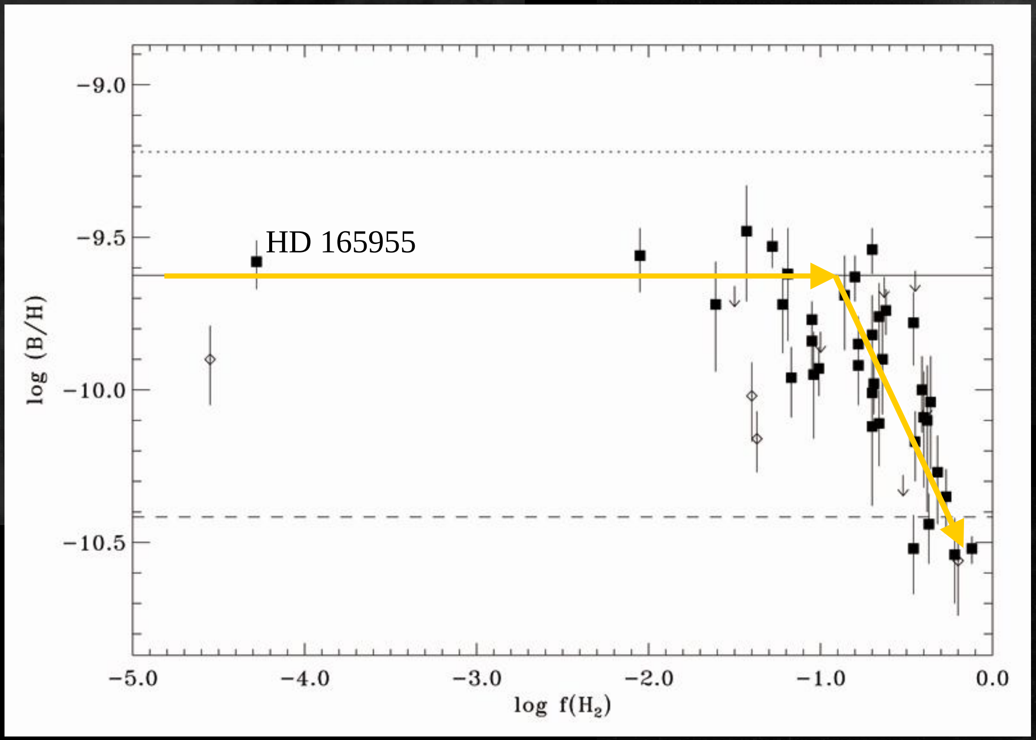

→ log ε(B) for HD 165955: 2.42 ± 0.08

→ average for warm gas: 2.38 ± 0.10

Galactic Evolution of Boron

Stellar Halo and Disk Abundances:

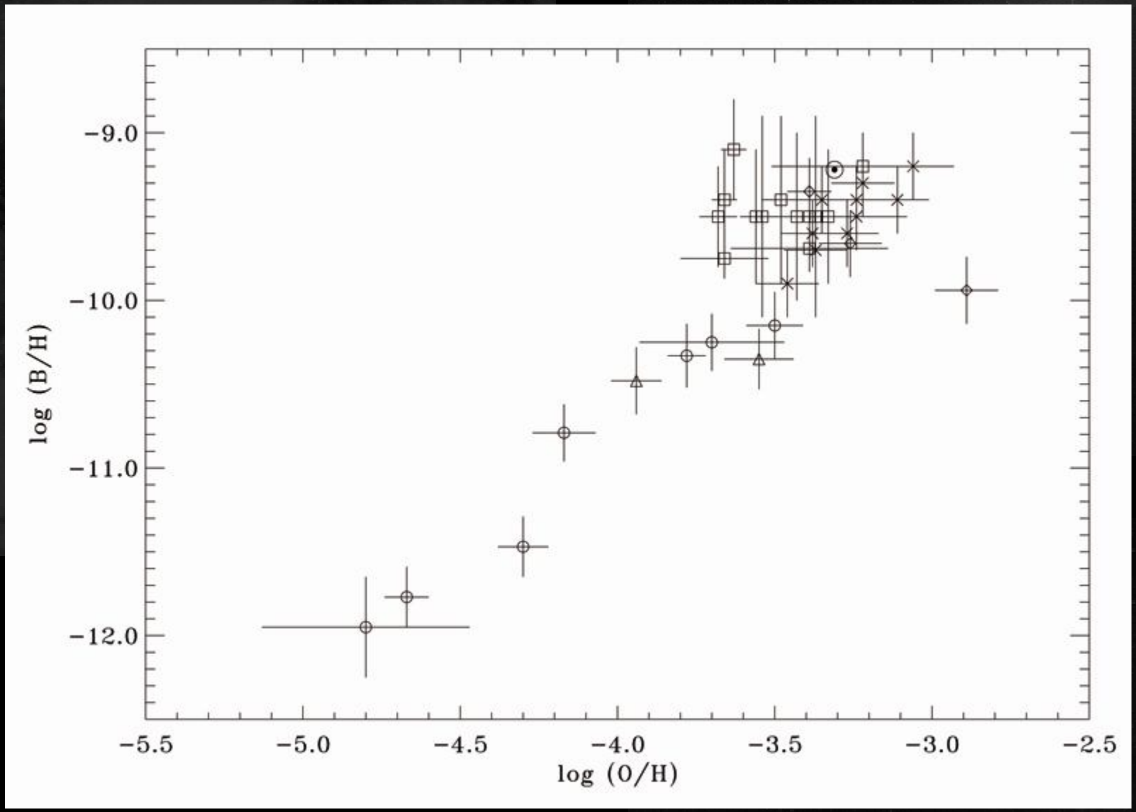

Galactic Evolution of Boron

Stellar Halo and Disk Abundances (+ ISM):

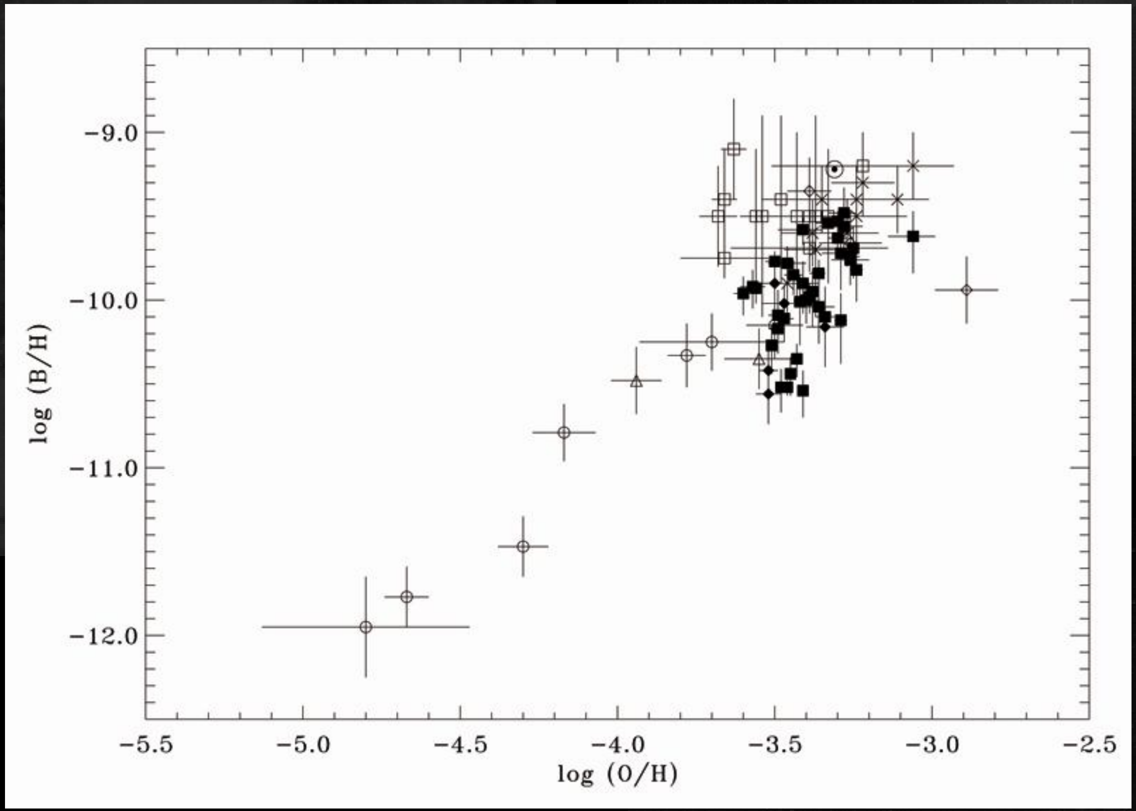

Galactic Evolution of Boron

Stellar Halo and Average Disk Abundances (+ Average Warm ISM):

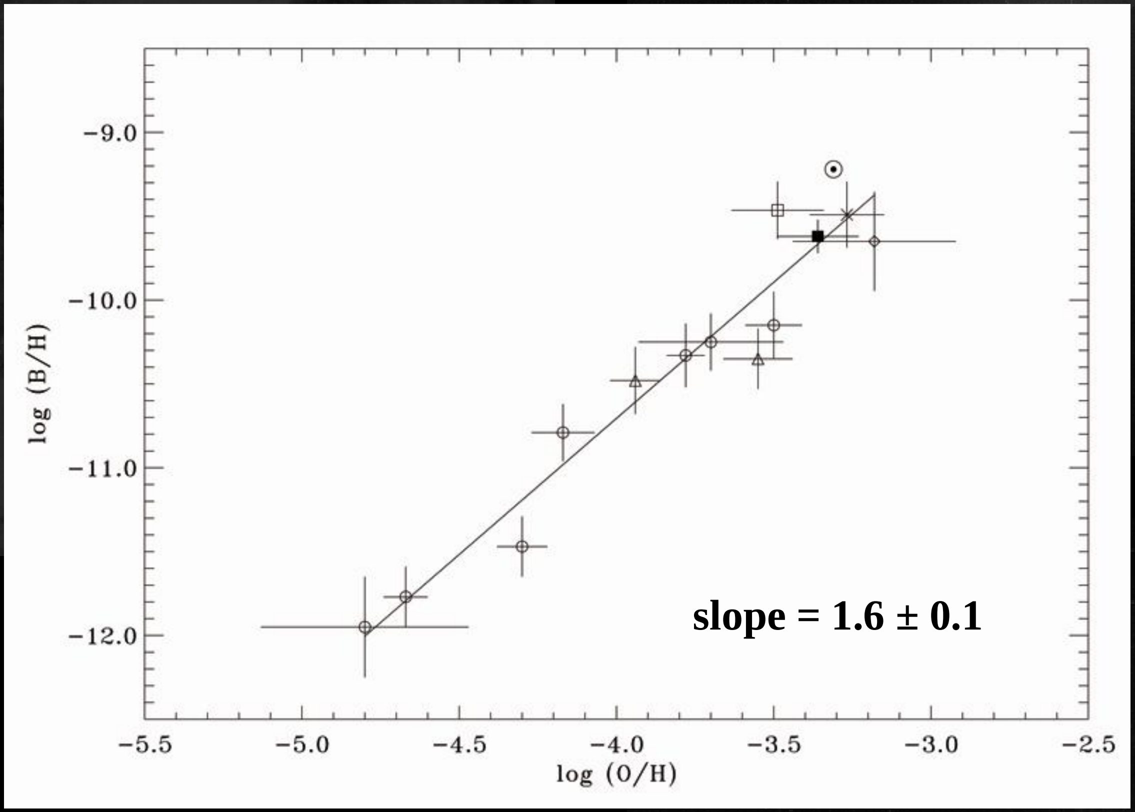

log ε(B) =

Solar:
2.78 ± 0.04

B stars:
2.54 ± 0.17

F, G stars:
2.51 ± 0.20

ISM (warm):
2.38 ± 0.10

G stars (Orion):
2.35 ± 0.30

Galactic Evolution of Boron

Stellar Halo and Average Disk Abundances (+ Average Warm ISM):

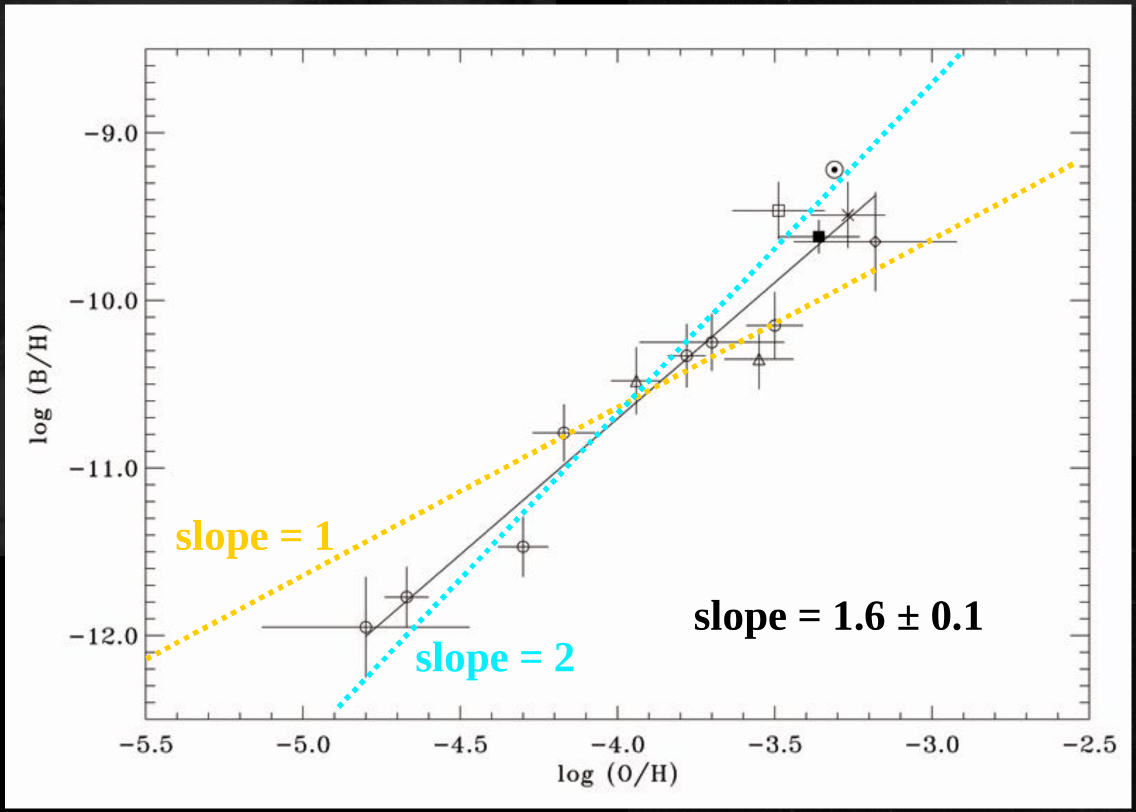

log ε(B) =

Solar:
2.78 ± 0.04

B stars:
2.54 ± 0.17

F, G stars:
2.51 ± 0.20

ISM (warm):
2.38 ± 0.10

G stars (Orion):
2.35 ± 0.30

→ Reverse spallation
→ Primary mechanism

→ Forward spallation
→ Secondary mechanism

Local Enhancements in B/H?

Recent production of ^{11}B by cosmic-ray or neutrino-induced spallation, expected in regions where Type II supernovae have occurred, will enhance B/H locally.

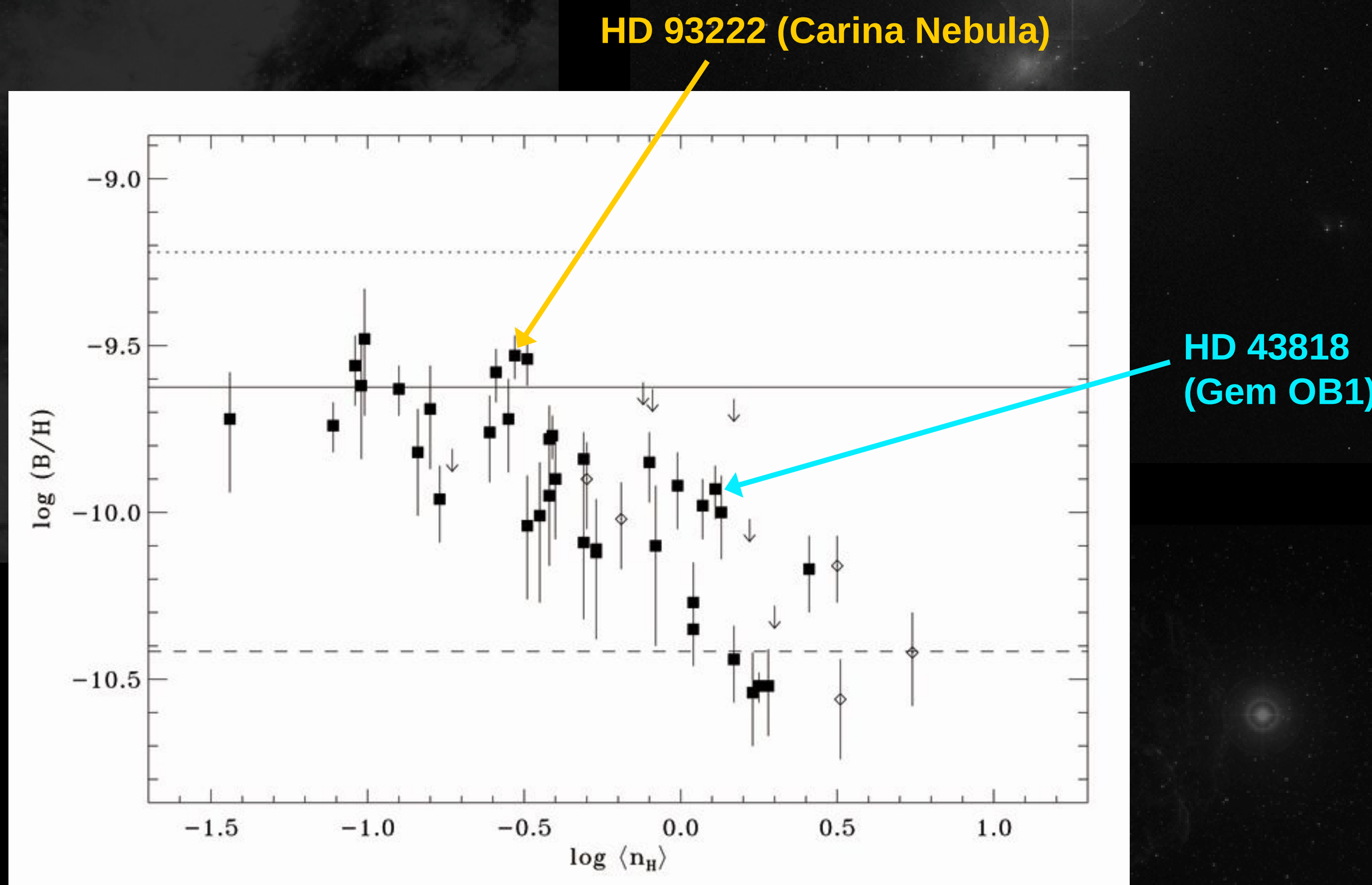

Local Enhancements in B/H?

HD 93222: B/H enhanced by 0.27 dex relative to sight lines with same average density.

Walborn et al. (2007) discuss expanding structures seen in interstellar absorption lines in the context of a possible SNR in this direction.

→ highest known interstellar velocities in the nebula occur in the spectrum of HD 93222.

Optical image of the Carina Nebula (DSS)

***Hubble Space Telescope* ACS/WFC (NASA, ESA, Hubble Heritage Team)**

Local Enhancements in B/H?

HD 43818: B/H enhanced by 0.26 dex relative to sight lines with same average density.

Acciari et al. (2009): suggest cosmic ray interactions with a molecular cloud to explain extended VHE gamma-ray emission.

→ we are pursuing ^{7}Li/^{6}Li ratios and Li and Rb abundances toward stars closer to the SNR.

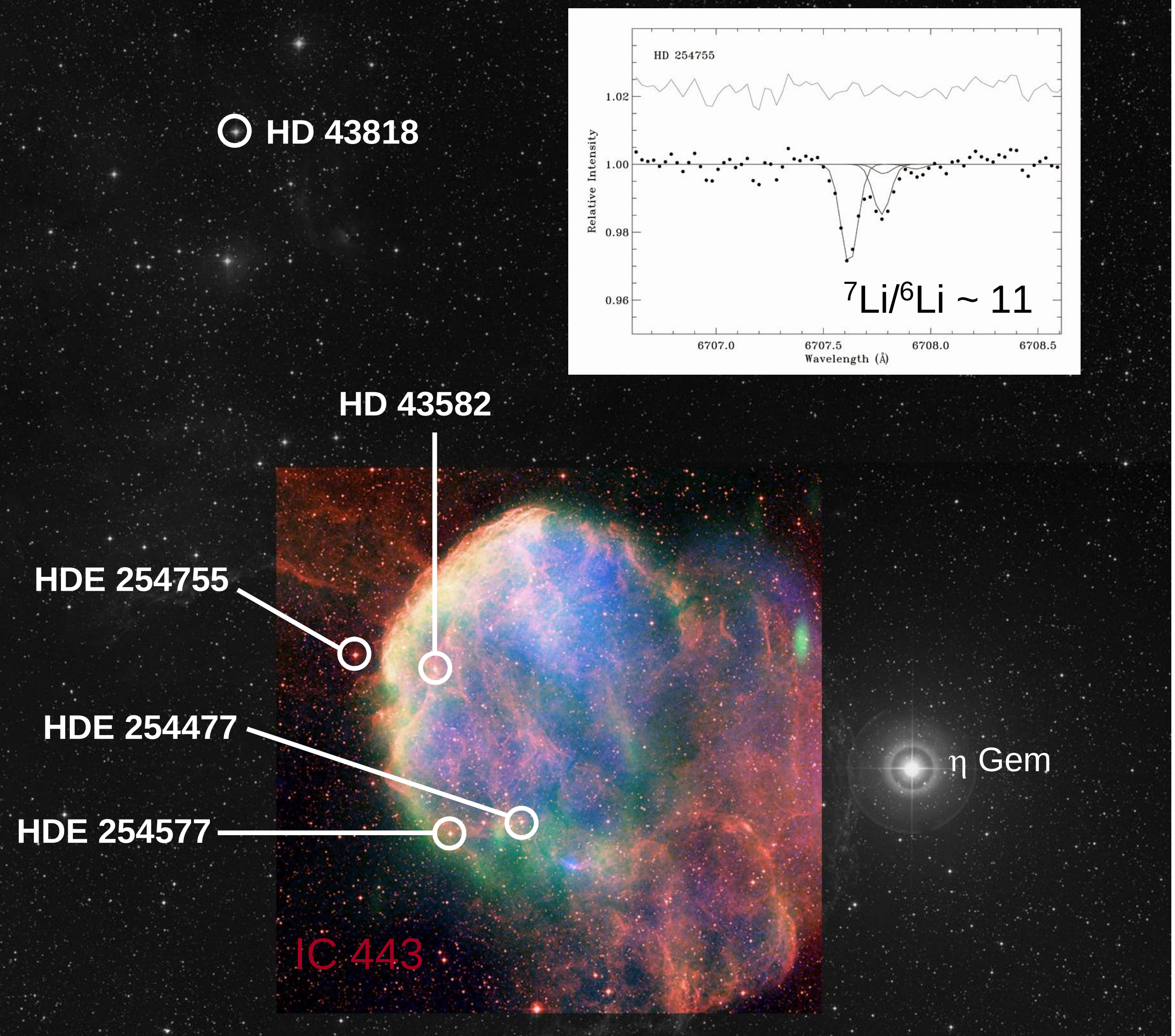

Optical image of IC 443/Gem OB1 (DSS)   Chandra X-ray (NASA/CXC), ROSAT X-ray (NASA/ROSAT), Radio (NRC/DRAO)

Local Enhancements in B/H?

o Per: B/H enhanced by 0.18 dex relative to the three other sight lines in Per OB2.

Federman et al. (1996): infer an enhanced cosmic ray flux toward o Per based on measurements of interstellar OH.

Knauth et al. (2000, 2003): detect a low $^{7}Li/^{6}Li$ ratio in at least one component toward o Per.

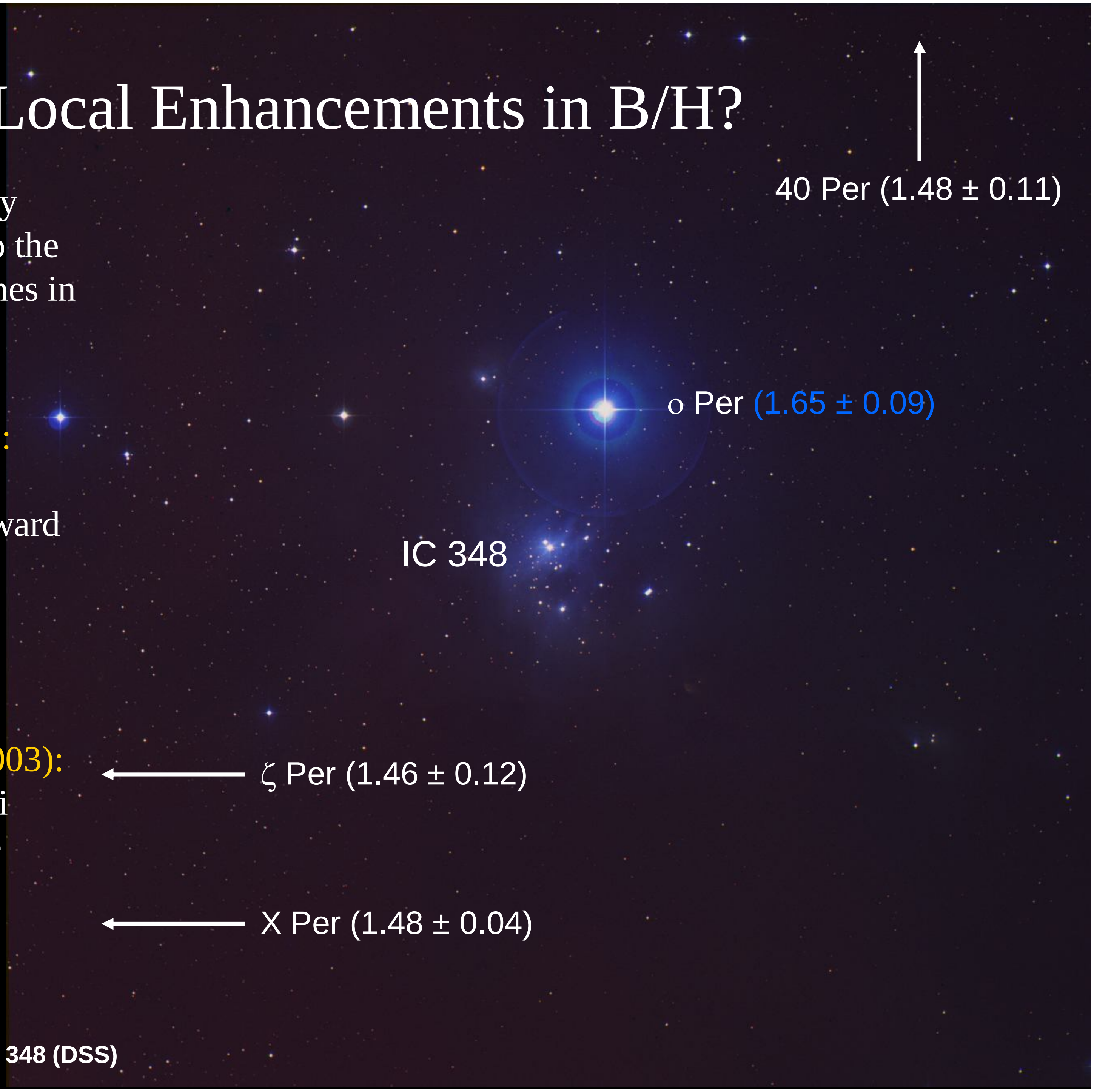

Color composite image of IC 348 (DSS)

Interstellar Fluorine-to-Boron Ratio

^{19}F synthesized by the ν-process, yet not produced in significant quantities by cosmic rays.

Supernova yields from a 25 M_{sun} progenitor result in F/B ratio of 42 (Woosley & Weaver 1995).

Only three sight lines have both fluorine and boron measurements:

	F/B
δ Sco	178
HD 177989	145
HD 209339	214

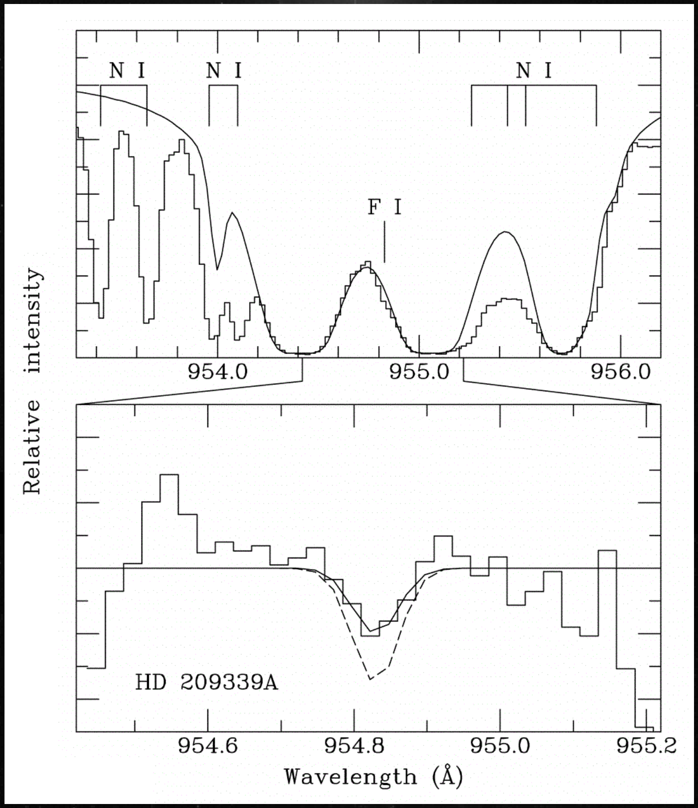

Federman et al. 2005

→ no evidence of ν-process in Cep OB2, a region shaped by past supernovae (?)

Interstellar LiBeB Abundances

	log ε(Li)	log ε(Be)	log ε(B)	Li/B	B/Be
ISM					
o Per	2.45 ± 0.16	…	1.65 ± 0.09	6.3	…
ζ Per	2.52 ± 0.07	< −0.15	1.46 ± 0.12	11.4	> 40
X Per	1.80 ± 0.14	…	1.48 ± 0.04	2.1	…
δ Sco	…	< 0.92	1.84 ± 0.09	…	> 8
ζ Oph	2.60 ± 0.14	< 0.78	1.44 ± 0.12	14.7	> 5
Solar	3.28 ± 0.06	1.41 ± 0.08	2.78 ± 0.04	3.2	23
GCR	2.30	1.30	2.48	0.66	15

→ elemental ratios difficult to interpret due to uncertain corrections for depletion.

Interstellar Depletion vs. T_C

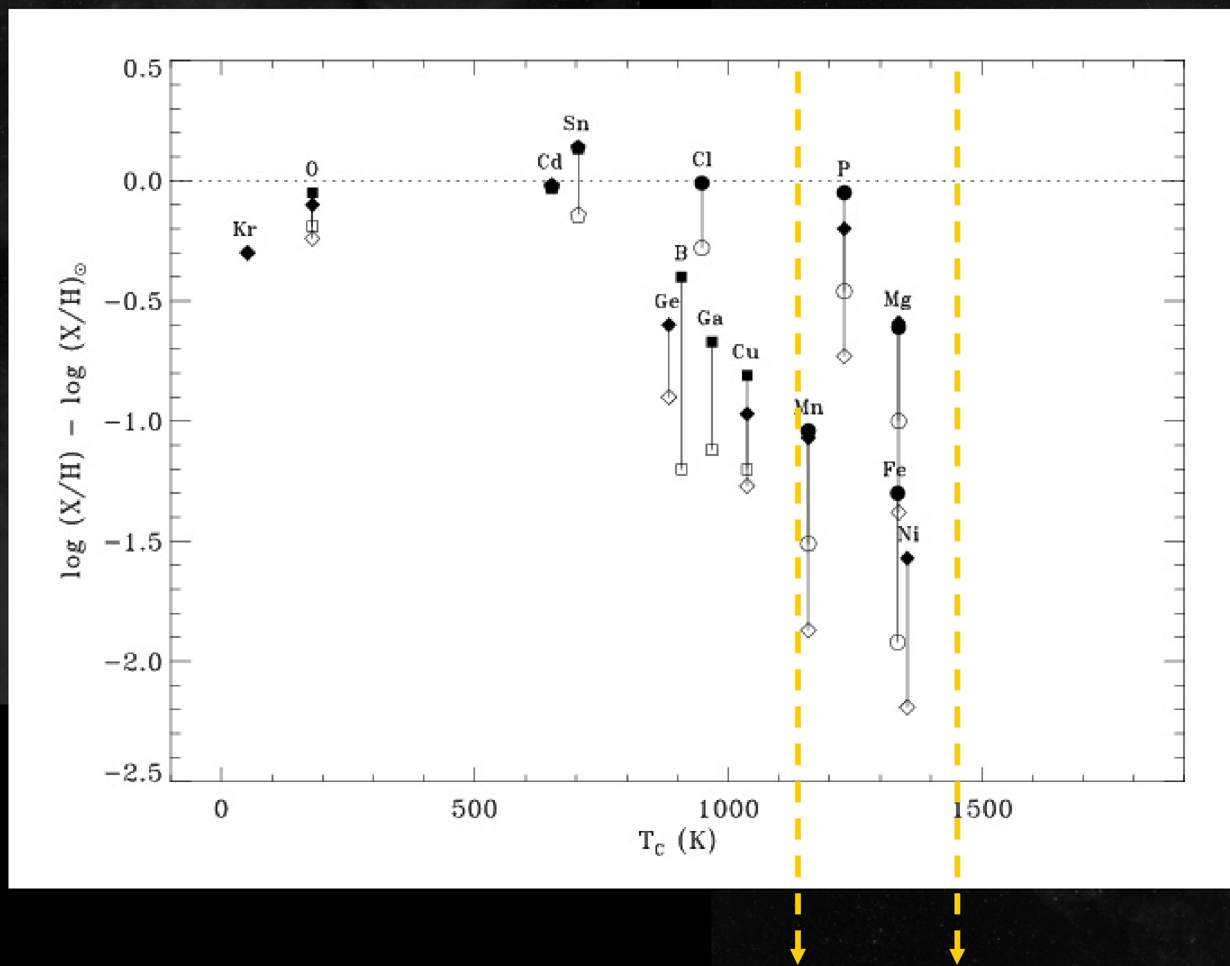

Li
$T_C = 1142$

Be
$T_C = 1452$

Conclusions

56 sight lines from STIS were analyzed to determine elemental abundances of boron (as well as oxygen, copper, and gallium).

Clear trend of depletion found for all species and average abundances were determined for warm and cold phases of the ISM.

Boron abundance in low-density warm gas (2.38 ± 0.10) consistent with abundances in a variety of Galactic disk stars. Stellar and interstellar values all significantly lower than solar system value.

Elevated B/O ratios in Sagittarius-Carina spiral arm may indicate the secondary nature of Galactic boron production in the current epoch.

Sight lines with enhanced B/H ratios potentially trace recent production of ^{11}B by cosmic-ray or neutrino-induced spallation.

Future Work

→ pursue ^{7}Li/^{6}Li ratios to determine whether there is enhanced ^{7}Li where B/H is elevated. Both cosmic-ray and neutrino-induced spallation produce ^{11}B and ^{7}Li.

→ extend the examination of boron abundances to the LMC/SMC with the newly refurbished STIS. The Magellanic Clouds provide an opportunity to study light element synthesis in metal-poor environments in regions of active star formation yielding clues to the dominant mechanisms of LiBeB production in our own Galaxy at earlier times.

→ detection of beryllium in interstellar space (via the Be II doublet at λ3130) will be an important milestone in cosmochemistry. Beryllium is a factor of 20 less abundant than boron and depletion will be more severe. Thus, sight lines must be chosen that have the least depletion. Still, equivalent widths likely to be < 0.1 mÅ.

ACKNOWLEDGEMENTS:

S. R. Federman (Univ. of Toledo)

Y. Sheffer (Univ. of Maryland)

D. L. Lambert (Univ. of Texas)

J. C. Howk (Notre Dame)

D. E. Welty (Univ. of Illinois)

STIS Help Desk

This research was funded by the Space Telescope Science Institute (STScI) through grant HST-AR-11247.01-A.